NASA TECHNICAL NOTE

NASA TN D-7779

NASA TN D-7779

MINIMUM-WEIGHT DESIGNS FOR HAT-STIFFENED COMPOSITE PANELS UNDER UNIAXIAL COMPRESSION

by Banarsi Agarwal and Randall C. Davis

Langley Research Center
Hampton, Va. 23665

NATIONAL AERONAUTICS AND SPACE ADMINISTRATION • WASHINGTON, D. C. • NOVEMBER 1974

MINIMUM-WEIGHT DESIGNS FOR HAT-STIFFENED COMPOSITE PANELS UNDER UNIAXIAL COMPRESSION

By Banarsi Agarwal and Randall C. Davis
Langley Research Center

SUMMARY

Optimum hat-stiffened compression panel designs are determined using a structural synthesis technique. Effects of simplifying assumptions made in the buckling analysis for the optimization program are investigated using a more accurate analysis which is a linked plate element program. Optimization results for an aluminum panel are compared with available results. Optimization results for hat-stiffened graphite-epoxy panels show a 50-percent weight savings over optimized aluminum panels. Using the structural synthesis technique, composite panels are shown to possess a variety of proportions at nearly constant weight.

INTRODUCTION

Optimization of structural members has been a necessary research objective in the past (refs. 1 to 12). The need for highly efficient structures in the aerospace industry led to the development of fiber-reinforced composite materials. The low density and high stiffness of these materials, relative to conventional aerospace metals, indicated that they would be highly efficient in compression members, and that the optimum proportions of such structures should be investigated.

Past investigators (refs. 13 to 19) have used various techniques to determine optimum proportions for structural elements constructed from conventional isotropic metals. These techniques, for many reasons, are insufficient for the optimum design of composite structural elements. Unlike conventional metals, filamentary reinforced composite materials are orthotropic, or even anisotropic. The full determination of the appropriate form and optimum proportions of structural elements using these materials requires consideration of significantly larger numbers of design variables than do isotropic designs. Imposing undue restrictions on the design process just to effect a simpler solution to the optimization problem denies the designer many of the advantages offered by using composite materials. Therefore, the purpose of this paper is to present optimized designs for hat-stiffened graphite-epoxy compression panels, obtained using an optimization technique which can efficiently handle a large number of design variables.

In this study, a nonlinear mathematical programming technique (ref. 20) called AESOP (Automated Engineering and Scientific Optimization Program) was used in conjunction with a stiffened-panel mathematical model to determine optimum composite panel designs. Optimum stiffened designs were also generated using aluminum properties for comparison with the graphite-epoxy results and published aluminum designs.

The mathematical model of the stiffened panel considered both stability and strength of the panel elements. Local stability of the panel elements was described by orthotropic plate theory. Overall panel stability (Euler buckling) was described using wide-column theory. A simplified maximum strain criteria was used to describe strength limitations of the graphite-epoxy material.

SYMBOLS

The units used for physical quantities defined in this paper are given in the International System (SI) of Units, except where noted. Correlations between this system of units and U.S. Customary Units are given in reference 21.

A	total cross sectional area of one pitch of the stiffened panel
A_i	area of the ith panel element
b	total panel width
b_i	width of the ith panel element
b_l	plate width
$\bar{b}_2$	projected depth of panel stiffener
D_{ij}	bending stiffness coefficients
E	Young's modulus
E_i	elastic modulus of the ith panel element
EI	effective bending stiffness of the panel
E_l	principal lamina modulus in the direction of loading

E11	lamina modulus in the filament direction
E22	lamina modulus transverse to the filament direction
f_i	percentage of $\pm 45^o$ material in the ith panel element
G12	lamina inplane shear modulus
I_{o_i}	moment of inertia of the ith panel elements about its centroid
i,j	indices
L	length of the panel
N_x	applied load per unit width of the panel
$N_{x_{Euler}}$	Euler buckling load per unit width of the panel
P_{a_i}	applied load on the ith panel element
P_{l_i}	local buckling load of the ith panel element
P	total load on the panel per unit pitch
t	plate thickness
t_i	thickness of the ith panel element
t_l	lamina thickness
W	panel mass
$\bar{y}$	distance of the neutral axis from the reference axis
y_i	distance of centroid of the ith panel element from the reference axis
ϵ	strain in the panel
ϵ_a	allowable strain

ν Poisson's ratio

$\nu 12$ lamina transverse Poisson's ratio

ρ material density

$\bar{\rho}$ mass per unit area

ϕ performance function

σ_{a_i} stress applied to the ith panel element

σ_l local buckling stress

Subscript:

i ith panel element

Superscripts:

L lower bound

H upper bound

ANALYSES

The general optimization cycle used is depicted in figure 1. The synthesis model consists of two parts, namely, the mathematical model and the optimizer. The mathematical model describes the strength and stability idealization of the structure to be optimized and a structural analysis of the mathematical model determines the design variables. The performance function is evaluated for these design variables and checked for optimality. The design variables are incremented, in accordance with the optimization scheme, subject to various constraints and the process is repeated until an optimum design has been generated. Details of the optimization scheme are given in appendix A.

The problem considered herein is the optimization of a hat-stiffened composite panel under uniaxial compression. The loaded edges of the panel are simply-supported and the unloaded edges are free. Figure 2 shows a schematic drawing of such a panel. Properties of the graphite-epoxy and aluminum material used in this study are given in table 1.

Mathematical Model

Basic assumptions.- The following basic assumptions are noted:

(1) Panel elements for the local buckling analysis are orthotropic constant-thickness plates, simply supported on all four edges.

(2) The panel is assumed to behave like a wide column for the overall or Euler buckling analysis.

(3) Twisting (or torsional) failure modes of the stiffeners are not considered.

(4) Two kinds of orthotropic lamina are used, namely, 0° lamina and a lamina with the extensional properties of a $\pm 45^{\circ}$ laminate.

(5) Bending-twisting coupling effects in the composite material are not considered.

(6) Each panel element is assumed to have no more than three layers, stacked in a balanced and midplane symmetric manner. Either 0° or $\pm 45^{\circ}$ material is permitted as the outside laminae.

(7) Allowable strain in compression for any panel element is conservatively set equal to the yield strain of the 0° composite material irrespective of the percentage of $\pm 45^{\circ}$ material contained in the panel element.

Design variables.- Under the assumption of wide-column behavior, only one pitch of the stiffener spacing is required for analysis. Figure 3 shows a representative cross section of the idealized panel and details the design variables used. For the hat-stiffened configuration the design variables are:

b_i width of panel element

t_i thickness of panel element

f_i percentage of $\pm 45^{\circ}$ material in panel element where $i = 1, 2, 3, 4$

Performance function.- The performance function used in this analysis is a weight parameter defined as mass per unit width of the panel

$$\phi = \frac{\bar{\rho} A}{(b_1 + 2b_4)} \tag{1}$$

Constraints.- In order to complete the definition of the problem, geometric and strength constraints must be specified. Those selected for this study are:

(1) Local buckling load of each panel element shall be greater than or equal to the applied load,

$$P_{l_i} \geq P_{a_i} \tag{2}$$

(2) Euler buckling load of the total panel shall be greater than or equal to the applied loading,

$$N_{x_{Euler}} \geq N_x \tag{3}$$

(3) Applied strain of the total panel shall be less than or equal to the allowable strain,

$$\epsilon \leq \epsilon_a \tag{4}$$

(4) Stiffener spacing shall be greater than or equal to b_3 (see fig. 3),

$$b_1 + 2b_4 \geq b_3 \tag{5}$$

(5) The value of the design variables shall be limited to a region of practical interest,

$$\left.\begin{aligned} b_i^L &\leq b_i \leq b_i^H \\ t_i^L &\leq t_i \leq t_i^H \\ f_i^L &\leq f_i \leq f_i^H \end{aligned}\right\} \tag{6}$$

For this study these limits are:

$$\left.\begin{aligned} 0.762 &\leq b_i \leq 25.4 \text{ cm} \\ 0.00254 &\leq t_i \leq 1.27 \text{ cm} \\ 0 &\leq f_i \leq 100 \text{ percent} \end{aligned}\right\} \tag{7}$$

The values of the load and strain parameters in equations (2) to (4) are determined through a simplified buckling analysis discussed in detail in appendix B.

RESULTS AND DISCUSSION

Using the synthesis model described above, optimum designs for graphite-epoxy and aluminum panels are generated at various load levels. Results are summarized in figure 4, which is a standard weight-strength plot of the strength parameter N_x/L and the weight parameter W/bL^2. Results for the composite and aluminum panels are shown as solid lines. The broken lines are the material strength limits for the aluminum and the graphite-epoxy material.

Aluminum Panels

Results from reference 2 for an aluminum panel are presented in figure 4 for comparison. As shown, the present results for an aluminum panel show a slight advantage over the results of reference 2. In reference 2 the flange width, cap width, and stiffener height are arbitrarily set to be a percentage of the width b_1 of the stiffener to effect an easier solution. No such simplifying assumptions with respect to the cross section are used in the present study, hence the optimum panel designs show a slight advantage over those of reference 2.

Also, reference 2 uses the optimization condition that local buckling in each panel element be coincident with Euler buckling of the whole panel. In the present analysis no such condition is imposed. However, results of the optimization process show that, in fact, for the optimum aluminum design, local buckling of each element and Euler buckling of the entire panel should occur simultaneously.

Graphite-Epoxy Panels

An attempt was made to compare results obtained for graphite-epoxy panels with similarly optimized composite panels in the literature, however, no published results could be found. Therefore, to assess the accuracy of the procedures used, a study is made of the effects of the simplifying assumptions employed in the present buckling analysis. This is done by determining the buckling load for a set of optimized panels using BUCLASP-2 (refs. 22 and 23), a computer program which is devoid of all such assumptions, with the exception that bending-twisting coupling is ignored. The BUCLASP-2 buckling loads are then plotted against the optimum value of the weight parameter. These points, shown as circles in figure 4, show good agreement with the present results. It is also noted that for the composite panel, results obtained using BUCLASP-2 show that local buckling and Euler buckling of the optimized panel occur at very nearly the same load.

The results in figure 4 show that optimized graphite-epoxy panel designs weigh approximately one-half as much as optimized aluminum designs over a wide loading range. Thus, such panels have a significant potential for lightweight aircraft or spacecraft compression structures.

An important result of the present study is illustrated in figure 5 which shows two composite panel cross sections that weigh approximately the same at both a high and a low load. The design variables for a range of loadings that show this phenomenon are detailed in tables 2 to 5 and differ markedly. This result has fortuitous ramifications when manufacturing constraints are considered, indicating that some design variables could be fixed for manufacturing reasons without adversely affecting the efficiency of the panel.

However, one should make sure in such cases that the extreme designs do not come about because of assumptions made during the buckling analysis and, in reality, fail in a neglected mode. For example, figure 6 shows the buckling mode shapes for the two highly loaded panels in figure 5. These mode shapes were obtained from BUCLASP-2. The panel in figure 6(b) fails in a local buckling mode and all the panel members behave as simply supported elements, which is in accord with the simplifying assumptions. The stiffener in figure 6(a) is very deep, compared to its width, and fails in a twisting, or torsional mode, 10 percent below the optimum design value. This mode of failure was neglected in the mathematical-model stability analysis. Alternate designs which are very similar to that of figure 6(a) but do not exhibit the torsional mode of failure can be found in tables 2 to 5.

The panel shown in figure 5(b) has 100 percent $\pm 45^{\circ}$ material in the skin and in the stiffener webs. Also, the optimized thickness of the webs and skin is very small compared to the thickness of the stiffener cap and flanges (see tables 2 to 7). This suggests that most of the load is carried by the 0° material, which results in a more efficient panel. It is significant that, in general, the optimization procedure found designs with 100 percent 0° material in the flanges and stiffener caps and 100 percent $\pm 45^{\circ}$ material in the webs. This suggests a method of reinforcing conventional metal hat-stiffened panels with composites by bonding unidirectional material to the flange and stiffener cap. In practice this is indeed the case if the composite material is compatible with the metal in the panel. It should be noted in figure 5 that the amount of $\pm 45^{\circ}$ material in the skin ranges from 0 to 100 percent. Only the two extreme cases, however, are shown in the figure.

Practical Constraints

Results presented in figure 4 and tables 2 to 8 give the optimized values of the different design variables for the composite and the aluminum panels; examination of these results reveals that they are not very practical from a manufacturing point of view. In the case of the aluminum panels it is more practical to have a constant stiffener thickness (i.e., $t_2 = t_3 = t_4$ (see fig. 3)). The effect of imposing such a constraint in the optimization procedure on the aluminum panel is shown in figure 7. It can be seen that an approximate 10-percent weight penalty is paid in using such a constraint.

In the case of the composite panel it is not practicable to make a hat stiffener with only 0° material in the stiffener cap. A more practical design, shown in figure 8, eliminates the problem of bonding the 0° cap material to the $\pm 45^{\circ}$ material in the webs. The 0° material for the cap is encapsulated by the $\pm 45^{\circ}$ material which makes up the stiffener webs. The effect of placing such a constraint on the optimum panel is shown in figure 9 and, as can be seen, only a very nominal penalty is incurred. If practical constraints are included in the optimization process, the composite material appears to give more flexibility to the design process with little penalty. Values of the optimized design variables for the composite panel with practical constraints are presented in table 9. Specifying the orientation of the material comprising the various plate elements, as shown in figure 8, eliminates f_i as a design variable and reduces the total number of variables from 12 to 8.

Variable Sensitivity

An apparent insensitivity of the weight parameter W/bL^2 to design-variable change was investigated in detail to define limits for certain design variables. Results of studies of the variables b_1 and b_3 are shown in figures 10 and 11, respectively. These figures are obtained for the fixed value of N_x/L equal to 2069 kPa.

The plot of W/bL^2 and b_1 in figure 10 is obtained by specifying b_1 during an optimization cycle while the other design variables remain unspecified. Since previous optimization results always give the same values for f_2, f_3, and f_4, these values were also held fixed, leaving f_1 free to vary. A similar approach was used for the results in figure 11. Figures 10 and 11 show that the weight parameter is relatively insensitive to independent changes in either b_1 or b_3 over a wide range (shown by the hatched area). This demonstrates that considerable freedom exists for a designer to specify practical dimensional constraints without incurring any weight-parameter penalty. Optimum construction for the panel skins was also found to be a function of b_1 and b_3. The variable f_1 varied from 0 percent for the narrow stiffener design to 100 percent for the wide stiffener.

CONCLUDING REMARKS

A mathematical model including both strength and stability effects, for hat-stiffened compression panels has been developed. This model was combined with a nonlinear mathematical programming technique and used to generate optimum designs for both graphite-epoxy and aluminum panels. Selected optimum designs were analyzed with a more complete stability analysis which was devoid of assumptions used in the synthesis model. Based on the analytical results presented herein, the following conclusions can be made:

1. Optimized graphite-epoxy panels weigh approximately one-half as much as optimized aluminum panels over a wide loading range.

2. Composite panel designs can be evolved via the optimization procedure which weigh essentially the same, but have geometric proportions which differ markedly.

3. Introduction of practical constraints as design variables can in some cases result in panels which are easier to manufacture and which will only weigh 10 percent more than optimum.

4. In order to ensure that complex failure modes will not cause premature failure, optimized designs should be reanalyzed with methods which are devoid of the simplifying assumptions incorporated in the synthesis model.

Langley Research Center,
National Aeronautics and Space Administration,
Hampton, Va., September 16, 1974.

APPENDIX A

DESIGN SYNTHESIS PROGRAM

This appendix is devoted to discussing the design synthesis program developed for the purpose of optimizing the weight parameter of a composite hat-stiffened panel under uniaxial compression.

Figure 12 shows a schematic flow chart of the optimization computer program AESOP (Automated Engineering and Scientific Optimization Program). (See ref. 20.) There are nine search algorithms available in AESOP, for the purpose of seeking a minimum solution. One or a combination of search algorithms can be used for this purpose. For the present work a combination of adaptive creep search and pattern search was found to be most efficient and effective in terms of computation and, hence, was used for the optimization work. Resulting typical CPU times for a single panel-optimization run on the CDC 6600 computer were about 10 seconds.

The AESOP computer program requires a user-defined subroutine describing the problem to be minimized. The hatched area in figure 12 represents subroutine PANEL developed for the present problem. A listing of subroutine PANEL is given at the end of this appendix. It should be noted that subroutine PANEL has been developed only for the composite hat-stiffened panel. In order to use this program for any other kind of panel it would have to be modified.

Subroutine PANEL employs the user-defined subroutines SIGEULR and SIGLOCL which compute the Euler buckling stress and the local buckling stress, respectively. Listings of these subroutines are also given with the listing of PANEL.

```
      SUBROUTINE PANEL
      COMMON/AESOPD/ADATA(5000)
      COMMON/SLOCAL/F(5,2),NN,IA(2,6),NSEQ(16,6),FCFIVE(6),ALPH,BAA
     1,AK(5),CONST(5)
      COMMON/RTP/B(10),TT(5),PI,EX(6),BL,BA,SIGMA(10),AREA
      COMMON/LENGTH/AL,A(5)
      DIMENSION SIBAR(20),EPSL(6),AA(5),SIGA(5)
      REAL ALPHA(100)
      REAL FUNCTN(100)
      EQUIVALENCE(ADATA(3455),SIBAR)
      EQUIVALENCE(ADATA(742),ALPHA)
      EQUIVALENCE(ADATA(2552),FUNCTN)
      EQUIVALENCE(ADATA(2736),JJJ)
      EQUIVALENCE(ADATA(2948),MAXJJJ)
      TT(1)=ALPHA(1)
      TT(2)=ALPHA(2)
      TT(3)=ALPHA(3)
      TT(4)=ALPHA(4)
      B(1)=ALPHA(5)
      B(2)=ALPHA(6)
      B(3)=ALPHA(7)
      B(4)=ALPHA(8)
      PI=3.14159265358979
      ALPH=ATAN((B(1)-B(3))/(2*B(2)))
      BL=B(1)+2.*B(4)
      BA=B(2)-(TT(1)+TT(3)+TT(2))/2.
      B(6)=BA/COS(ALPH)
      BAA=B(2)
    1 FORMAT(5F10.3)
    2 FORMAT(F10.5,2I5)
    3 FORMAT(16I5)
    7 FORMAT(5F10.5)
      IF(JJJ.NE.1) GO TO 20
      READ 2,SIGMA(8)
      READ 2,AL,MN,KIK
      IF(KIK.NE.1) GO TO 20
      READ 1 ,((F(I,J),I=1,5),J=1,2)
      READ 7,(AK(I),I=1,MN)
   20 DO 100 NN=1,MN
      IF(KIK.NE.1) GO TO 25
      IF(JJJ.NE.1) GO TO 25
      READ 3,IA(1,NN),IA(2,NN)
```

```
      READ 3,(NSEQ(I,NN),I=1,16)
   25 CALL SIGLOCL
  100 CONTINUE
      AREA=PL*TT(1)+2.*B(4)*(TT(4)+TT(2))+2.*B(6)*TT(2)+B(3)*(TT(3)+
     1 TT(2))
      CALL SIGEULR
      EX(6)=EX(1)*A(5)/AREA
      DO 5 I=1,MN
      FUNCTN(I)=STBAR(I)
       SIGA(I)=EX(I)*BL*SIGMA(8)/(EX(6)*AREA)
      EPSL(I)=SIGA(I)/EX(I)
      IF(EPSL(I).GT..00575) FUNCTN(I)=(EPSL(I)-.00575)
    5 CONTINUE
      DO 15 I=1,MN
      FUNCTN(MN+I)=STBAR(MN+I)
      IF(SIGA(I).GT.SIGMA(I))FUNCTN(MN+I)=(SIGA(I)-SIGMA(I))
   15 CONTINUE
      FUNCTN(2*MN+1)=STBAR(2*MN+1)
      SIGMA(7)=SIGMA(6)*AREA/BL
      IF(SIGMA(7).LT.SIGMA(8))FUNCTN(2*MN+1)=(SIGMA(7)-SIGMA(8))
      FUNCTN(2*MN+2)=STBAR(2*MN+2)
      IF(BL.LT.B(3))FUNCTN(2*MN+2)=(BL-B(3))
      FUNCTN(2*MN+3)=AREA/BL
      IF((MAXJJJ+1).NE.JJJ) GO TO 30
   31 FORMAT(*1 LOCAL STRESS SIGMA(I)  * )
   32 FORMAT(*0 B(I)   *)
   33 FORMAT(*0 TT(I)   *)
   34 FORMAT(5E14.7)
   35 FORMAT(*0 EULER STRESS *)
   36 FORMAT(*0 AVERAGE LOADING*)
   37 FORMAT(*1FINAL RESULTS*)
   38 FORMAT(*0 LOCAL AVERAGE LOADING *)
   39 FORMAT(*0 LOCAL REAL STRESS *)
      PRINT 31
      PRINT 34,(SIGMA(I),I=1,MN)
      PRINT 39
      PRINT 34,(SIGA(I),I=1,MN)
      PRINT 35
      PRINT 34,SIGMA(6)
      PRINT 36
      PRINT 34,SIGMA(7)
      PRINT 32
      PRINT 34,(B(I),I=1,MN)
      PRINT 33
      PRINT 34,(TT(I),I=1,4)
   51 FORMAT( *0 EPSL(I) *)
      PRINT 51
      PRINT 34,(EPSL(I),I=1,4)
      PRINT 37
   30 RETURN
      END
```

```
      SUBROUTINE SIGLOCL
      COMMON/SLOCAL/E(5,2),NN,LA(2,6),NSEQ(16,6),FOFIVE(6),ALPH,BAA
     1,AK(5),CONST(5)
      COMMON/BTP/B(10),TT(5),PI,EX(6),BL,BA,SIGMA(10)
      DIMENSION T(2)
      REAL NUE
      IF (NN.EQ.1.OR.2) FOFIVE(NN)=100.
      IF (NN.EQ. 3) FOFIVE(NN)=100.*(TT(2)/(TT(3)+TT(2)))
      IF (NN.EQ.4) FOFIVE(NN)=100.*(TT(1)+TT(2))/(TT(1)+TT(2)+TT(4))
      SUM1=0
      SUM2=0
      SUM3=0
      SUM4=0
      SUM5=0
      DK=.5
      LLA=LA(1,NN)+LA(2,NN)
      IF(FOFIVE(NN) .GT. 100) FOFIVE(NN)=100.
      IF(FOFIVE(NN) .LT. 0) FOFIVE(NN)=0.0
      DO 100 I=1,LLA
      NE=NSEQ(I,NN)
      T(1)=(100.-FOFIVE(NN))/(100.*LA(1,NN))
      T(2)=FOFIVE(NN)/(100.*LA(2,NN))
      TTA=(4.*T(NE)**2-12.*DK*T(NE)+12.*DK**2)*T(NE)
      DK=DK-T(NE)
      NUE=1.-E(5,NE)*E(4,NE)
      SUMA1=E(1,NE)*TTA/NUE
      SUMA2=E(2,NE)*TTA/NUE
      SUMA3=E(1,NE)*E(5,NE)*TTA/NUE
      SUMA4=E(3,NE)*TTA
      SUMA5=E(1,NE)*T(NE)
      SUM1=SUM1+SUMA1
      SUM2=SUM2+SUMA2
      SUM3=SUM3+SUMA3
      SUM4=SUM4+SUMA4
      SUM5=SUM5+SUMA5
  100 CONTINUE
      EX(NN)=SUM5
      CONST(NN)=SQRT(SUM1*SUM2)+SUM3+2.*SUM4
      IF(NN.EQ.2) B(2)=B(6)
      IF (NN.NE.3) GO TO 10
      TT(3)=TT(3)+TT(2)
   10 IF(NN.NE.4) GO TO 1
      TT(4)=TT(4)+TT(1)+TT(2)
      B(4)=2.*B(4)
    1 SIGMA(NN)=AK(NN)*PI**2*(TT(NN)/B(NN))**2*CONST(NN)/6.
      B(2)=BAA
      IF (NN.NE.3) GO TO 20
      TT(3)=TT(3)-TT(2)
   20 IF(NN.NE.4) GO TO 2
      TT(4)=TT(4)-TT(1)-TT(2)
      B(4)=B(4)/2.
    2 RETURN
      END
```

```
      SUBROUTINE SIGEULR
      COMMON/LENGTH/ AL,A(5)
      COMMON/BTP/B(10),TT(5),PI,EX(6),BL,BA,SIGMA(10),AREA
      A(1)=B(1)*TT(1)
      A(2)=2.*BA*TT(2)*EX(2)/EX(1)
      A(3)=B(3)*(TT(3)+TT(2))*EX(3)/EX(1)
      A(4)=2.*B(4)*(TT(1)+TT(4)+TT(2))*EX(4)/EX(1)
      A(5)=A(1)+A(2)+A(3)+A(4)
      YBAR=(A(2)*B(2)/2.+A(3)*B(2)+A(4)*(TT(1)+TT(4)+TT(2))/2.)/A(5)
      B(7)=A(3)/(TT(3)+TT(2))
      B(8)=A(4)/(2.*TT(4)+TT(2)+TT(1))
      TT(5)=TT(2)*EX(2)/EX(1)
      XMOI=B(1)*TT(1)**3/12.+B(8)*(TT(1)+TT(2)+TT(4))**3/6.+B(7)*(TT(3)
     1 +TT(2))**3/12.+TT(5)*(B(2)-(TT(1)-TT(2)-TT(4))/2.)**
     23/6.+A(1)*YBAR**2+A(2)*(YBAR-B(2)/2.)**2+A(3)*(YBAR-B(2))**2+A(4)*
     3(YBAR-(TT(1)+TT(4)+TT(2))/2.)**2
      SIGMA(6)=EX(1)*PI**2*XMOI/(AL**2*AREA)
      RETURN
      END
```

APPENDIX B

BUCKLING ANALYSIS

The buckling analysis used is based on the variables for the cross section shown in figure 3. A similar analysis for the case presented in figure 8 can be performed by redefining the corresponding variables.

Load in Each Panel Element

Assuming N_x is the load intensity per unit width, σ_{a_i} is the axial stress in each panel element, and P is the total load per stiffener spacing, then,

$$P = N_x \cdot (b_1 + 2b_4) \tag{B1}$$

and

$$P = \sum_{i=1}^{4} \sigma_{a_i} A_i \tag{B2}$$

For compatibility, the strain in each panel element has to be equal. Hence

$$\epsilon = \frac{\sigma_{a_i}}{E_i} \qquad (i = 1,\ 2,\ 3,\ 4) \tag{B3}$$

where

$$E_i = \frac{\sum E_l t_l}{t}$$

and E_l is the principal lamina modulus calculated from the properties in table 1 through a standard lamina transformation formula (ref. 24). The Poisson effect neglected by this approach was found to be less than 0.5 percent. From equations (B2) and (B3)

$$P = \sum_{i=1}^{4} \epsilon E_i A_i$$

Solving this equation for the strain ϵ and using equation (B1)

$$\epsilon = \frac{N_x(b_1 + 2b_4)}{\sum_{i=1}^{4} E_i A_i} \tag{B4}$$

Finally the load P_{a_i} in each panel member is then given by

$$P_{a_i} = \sigma_{a_i} A_i = \frac{N_x b E_i A_i}{\sum_{i=1}^{4} E_i A_i} \tag{B5}$$

Local Buckling

Each panel member is assumed to be orthotropic and simply supported on all four edges. Hence, from orthotropic plate theory (ref. 25)

$$\sigma_l = \frac{2\pi^2}{b^2 t}\left(\sqrt{D_{11}D_{22}} + D_{12} + 2D_{66}\right) \tag{B6}$$

and

$$P_l = \sigma_l b_l t$$

where,

σ_l	local buckling stress
b_l	width of the plate
t	thickness of the plate
D_{ij}	bending stiffness coefficients
P_l	local buckling load

Here for the sake of simplicity the subscript i has been omitted. However, this equation applies to each panel element.

Euler Buckling

Only one pitch of stiffener spacing need be considered for the purpose of the Euler buckling analysis. Since each panel element can have a different percentage of $\pm 45^{\circ}$ laminates, each panel element will have a different value of Young's modulus. In order to find the Euler buckling load the equivalent area approach is used to find the effective Young's modulus and effective area of each panel element. Then

$$N_{x_{Euler}} = \frac{\pi^2 (EI)}{bL^2} \tag{B7}$$

where EI is the effective stiffness.

Assuming y_i is the distance of the center of gravity of the ith panel element from the reference axis (shown in fig. 3), E_i is the principal lamina modulus for the ith panel element, A_i is the area of the ith panel element, and $\bar{y}$ is the distance of the neutral axis from the reference axis, then,

$$\bar{y} = \frac{\sum_{i=1}^{4} E_i A_i y_i}{\sum_{i=1}^{4} E_i A_i} \tag{B8}$$

From figure 3 it can be seen that

$$\bar{b}_2 = \left[\left\{b_2 - \left(\frac{t_1 + t_4}{2}\right)\right\}^2 + \left(\frac{b_1 - b_3}{2}\right)^2\right]^{1/2} \tag{B9}$$

and

$$\left.\begin{aligned} A_1 &= b_1 t_1 \\ A_2 &= 2\bar{b}_2 t_2 \\ A_3 &= b_3 t_3 \\ A_4 &= 2b_4(t_1 + t_4) \end{aligned}\right\} \tag{B10}$$

Hence,

$$\bar{y} = \frac{\dfrac{E_2A_2b_2}{2} + E_3A_3b_2 + \dfrac{E_4A_4(t_1 + t_4)}{2}}{\displaystyle\sum_{i=1}^{4} E_iA_i} \tag{B11}$$

The effective EI of the cross section about the neutral axis can be written as

$$EI = \sum_{i=1}^{4} E_iI_{o_i} + \sum_{i=1}^{4} E_iA_i\bar{y}_i^2 \tag{B12}$$

where

I_{o_i} moment of inertia of the area of the ith panel element about its centroid

$\bar{y}_i$ distance of the centroid of the ith panel element from the neutral axis of the cross section

Hence,

$$\begin{aligned} EI = {} & \frac{1}{12} E_1(b_1 + 2b_4)t_1^3 + \frac{1}{6} E_2t_2\left[\frac{2\bar{b}_2}{2b_2 - t_1 - t_4}\right]\left[b_2 - \frac{1}{2}(t_1 + t_4)\right]^3 \\ & + \frac{1}{12} E_3b_3t_3^3 + \frac{1}{6} E_4b_4t_4^3 + E_1(b_1 + 2b_4)t_1\bar{y}^2 \\ & + E_2A_2\left(\bar{y} - \frac{1}{2} b_2 - \frac{t_4}{4}\right)^2 + E_3A_3(\bar{y} - b_2)^2 \\ & + 2E_4b_4t_4\left[\bar{y} - \frac{1}{2} (t_1 + t_4)\right]^2 \end{aligned} \tag{B13}$$

APPENDIX C

BUCLASP-2 ASSUMPTIONS AND MODEL

Effects of the simplifying assumptions in the buckling analysis were studied using the more accurate linked plate analysis program BUCLASP-2. This appendix is devoted to a discussion of some of the capabilities of BUCLASP-2 (a computer program for the instability analysis of biaxially loaded composite panels) as it pertains to the buckling analysis of the composite panels considered in the present work. This computer program (refs. 22 and 23) is operational on the CDC 6600 computer. Some of the basic assumptions made in the analysis of BUCLASP-2 are as follows:

(1) Panel elements are orthotropic and have balanced laminates.

(2) The material is linearly elastic.

(3) Thin-plate theory is employed.

(4) Effects of prebuckling deformations are ignored.

(5) Edges normal to the longitudinal direction are assumed to be simply supported.

Support conditions at other boundaries are arbitrary. With the above assumptions an "exact" analysis of the whole panel is made. This analysis results in the prediction of Euler buckling modes, local buckling modes, or coupled Euler and local modes.

The user of BUCLASP-2 has to define the mathematical model of the panel under consideration. This mathematical model consists of three substructures, namely, the start substructure, end substructure, and the repeat substructure. Figure 13 shows the cross sections of the three substructures for the panel studied in this investigation. The optimized panels studied using BUCLASP-2 in this work were seven stiffener spacings wide. The results after using AESOP define the cross-sectional dimensions of the panel. These dimensions are then used to find the buckling load using BUCLASP-2.

REFERENCES

1. Michell, A. G. M.: The Limits of Economy of Material in Frame-Structures. Phil. Mag. & J. Sci., sixth ser., vol. VIII, July-Dec. 1904, pp. 589-597.
2. Crawford, R. F.; and Burns, A. B.: Minimum Weight Potentials for Stiffened Plates and Shells. AIAA J., vol. 1, no. 4, Apr. 1963, pp. 879-886.
3. Cox, H. L.; and Smith, H. E.: Structures of Minimum Weight. R. & M. No. 1923, British A.R.C., 1943.
4. Schuette, Evan H.: Charts for the Minimum-Weight Design of 24S-T Aluminum-Alloy Flat Compression Panels With Longitudinal Z-Section Stiffeners. NACA Rep. 827, 1945. (Supersedes NACA WRL-197.)
5. Anderson, Melvin S.: Local Instability of the Elements of a Truss-Core Sandwich Plate. NASA TR R-30, 1959. (Supersedes NACA TN 4292.)
6. Seide, Paul; and Stein, Manuel: Compressive Buckling of Simply Supported Plates With Longitudinal Stiffeners. NACA TN 1825, 1949.
7. Gerard, George: Optimum Structural Design Concepts for Aerospace Vehicles. J. Spacecraft & Rockets, vol. 3, no. 1, Jan. 1966, pp. 5-18.
8. Morrow, William M., II; and Schmit, Lucien A., Jr.: Structural Synthesis of a Stiffened Cylinder. NASA CR-1217, 1968.
9. Hague, Donald S.: Application of the Variational Steepest-Descent Method to High Performance Aircraft Trajectory Optimization. NASA CR-73366, [1970].
10. Wilde, Douglass J.: Optimum Seeking Methods. Prentice-Hall, Inc., c.1964.
11. Fox, Richard L.: Optimization Methods for Engineering Design. Addison-Wesley Pub. Co., Inc., c.1971.
12. Emero, Donald H.; and Spunt, Leonard: Optimization of Multirib and Multiweb Wing Box Structures Under Shear and Moment Loads. AIAA 6th Structures and Materials Conference, Apr. 1965, pp. 330-353.
13. Becker, Herbert: The Optimum Proportions of a Multicell Box Beam in Pure Bending. J. Aeronaut. Sci., vol. 16, no. 11, Nov. 1949, pp. 653-658.
14. Becker, Herbert: The Optimum Proportions of a Long Unstiffened Circular Cylinder in Pure Bending. J. Aeronaut. Sci., vol. 15, no. 10, Oct. 1948, pp. 616-624.
15. Zahorski, Adam: Effects of Material Distribution on Strength of Panels. J. Aero. Sci., vol. 11, no. 3, July 1944, pp. 247-253.
16. Farrar, D. J.: The Design of Compression Structures for Minimum Weight. J. R.A.S., vol. 53, no. 467, Nov. 1949, pp. 1041-1052.

17. Shanley, F. R.: Weight-Strength Analysis of Aircraft Structures. McGraw-Hill Book Co., Inc., 1952.

18. Gerard, George: Efficient Applications of Stringer Panel and Multicell Wing Construction. J. Aeronaut. Sci., vol. 16, no. 1, Jan. 1949, pp. 35-40.

19. Gerard, George: Minimum Weight Analysis of Compression Structures. Interscience Publ., 1966.

20. Jones, R. T.; and Hague, D. S.: Application of Multivariable Search Techniques to Structural Design Optimization. NASA CR-2038, 1972.

21. Mechtly, E. A.: The International System of Units – Physical Constants and Conversion Factors (Revised). NASA SP-7012, 1969.

22. Viswanathan, A. V.; and Tamekuni, M.: Elastic Buckling Analysis for Composite Stiffened Panels and Other Structures Subjected to Biaxial Inplane Loads. NASA CR-2216, 1973.

23. Tripp, L. L.; Tamekuni, M.; and Viswanathan, A. V.: User's Manual – BUCLASP 2: A Computer Program for Instability Analysis of Biaxially Loaded Composite Stiffened Panels and Other Structures. NASA CR-112226, 1973.

24. Ashton, J. E.; Halpin, J. C.; and Petit, P. H.: Primer on Composite Materials: Analysis. Technomic Pub. Co., Inc., c.1969.

25. Timoshenko, S.: Theory of Elastic Stability. McGraw-Hill Book Co., Inc., 1936.

TABLE 1.- MATERIAL PROPERTIES

(a) SI Units

Graphite epoxy	Aluminum
E11 = 138 GPa	E = 68.9 GPa
E22 = 8.962 GPa	ν = 0.300
G12 = 4.48 GPa	ρ = 2768 kg/m^3
ν12 = 0.304	ϵ_a = 0.00575
ρ = 1522 kg/m^3	
ϵ_a = 0.00575	

(b) U.S. Customary Units

Graphite epoxy	Aluminum
E11 = 2×10^7 psi	E = 10^7 psi
E22 = 1.3×10^6 psi	ν = 0.300
G12 = 6.5×10^5 psi	ρ = 0.100 lb/in^3
ν12 = 0.304	ϵ_a = 0.00575
ρ = 0.055 lb/in^3	
ϵ_a = 0.00575	

TABLE 2.- OPTIMIZED DESIGN VARIABLES FOR GRAPHITE-EPOXY PANEL

$\left[f_1 = f_3 = f_4 = 0;\quad f_2 = 100;\quad L = 76.2 \text{ cm (30 in.)}\right]$

(a) SI Units

$\frac{N_x}{L}$, kPa	$\frac{W}{bL^2}$, kg/m^3	b_1, cm	b_2, cm	b_3, cm	b_4, cm	t_1, cm	t_2, cm	t_3, cm	t_4, cm
6895	141.0×10^{-1}	3.150	3.774	1.537	1.709	0.340	0.058	1.270	0.030
5516	120.3	2.449	3.835	1.524	1.524	.282	.064	.777	.041
3448	91.2	2.253	3.416	.762	1.407	.206	.048	1.128	.051
2758	81.3	1.986	3.251	.762	1.206	.175	.046	.879	.036
2069	68.8	1.976	3.353	.762	1.135	.168	.051	.498	.025
1379	56.4	1.549	3.048	.925	.932	.119	.043	.287	.025
690	40.4	1.361	2.718	.782	.871	.089	.033	.170	.025
345	29.6	1.346	2.210	.762	.914	.071	.025	.130	.025

(b) U.S. Customary Units

$\frac{N_x}{L}$, psi	$\frac{W}{bL^2}$, lb/in^3	b_1, in.	b_2, in.	b_3, in.	b_4, in.	t_1, in.	t_2, in.	t_3, in.	t_4, in.
1000	5.100×10^{-4}	1.240	1.486	0.605	0.673	0.134	0.023	0.500	0.012
800	4.350	.964	1.510	.600	.600	.111	.025	.306	.016
500	3.300	.887	1.345	.300	.554	.081	.019	.444	.020
400	2.940	.782	1.280	.300	.475	.069	.018	.346	.014
300	2.490	.778	1.320	.300	.447	.066	.020	.196	.010
200	2.040	.610	1.200	.364	.367	.047	.017	.113	.010
100	1.460	.536	1.070	.308	.343	.035	.013	.067	.010
50	1.070	.530	.870	.300	.360	.028	.010	.051	.010

TABLE 3.- OPTIMIZED DESIGN VARIABLES FOR GRAPHITE-EPOXY PANEL

$\left[f_1 = f_3 = f_4 = 0; \quad f_2 = 100; \quad L = 101.6 \text{ cm (40 in.)}\right]$

(a) SI Units

$\frac{N_x}{L}$, kPa	$\frac{W}{bL^2}$, kg/m^3	b_1, cm	b_2, cm	b_3, cm	b_4, cm	t_1, cm	t_2, cm	t_3, cm	t_4, cm
6895	143.8×10^{-1}	3.429	5.004	2.098	1.245	0.389	0.076	1.270	0.069
5516	127.2	1.651	5.055	1.168	1.600	.152	.076	1.270	.330
3448	91.2	2.146	4.648	.965	1.524	.246	.071	1.270	.038
2758	83.2	2.794	4.267	.991	1.697	.254	.058	1.270	.033
2069	68.6	2.591	4.191	.762	1.422	.216	.058	1.092	.025
1379	55.9	2.718	4.724	.762	1.600	.206	.058	1.255	.036
690	40.1	1.689	3.454	1.016	1.092	.112	.041	.259	.033
345	29.0	.952	3.048	.889	.889	.056	.033	.127	.046

(b) U.S. Customary Units

$\frac{N_x}{L}$, psi	$\frac{W}{bL^2}$, lb/in^3	b_1, in.	b_2, in.	b_3, in.	b_4, in.	t_1, in.	t_2, in.	t_3, in.	t_4, in.
1000	5.200×10^{-4}	1.350	1.970	0.826	0.490	0.153	0.030	0.500	0.027
800	4.600	.650	1.990	.460	.630	.060	.030	.500	.130
500	3.300	.845	1.830	.380	.600	.097	.028	.500	.015
400	3.010	1.100	1.680	.390	.668	.100	.023	.500	.013
300	2.480	1.020	1.650	.300	.560	.085	.023	.430	.010
200	2.020	1.070	1.860	.300	.630	.081	.023	.494	.014
100	1.450	.665	1.360	.400	.430	.044	.016	.102	.013
50	1.050	.380	1.200	.350	.350	.022	.013	.050	.018

TABLE 4.- OPTIMIZED DESIGN VARIABLES FOR GRAPHITE-EPOXY PANEL

$\left[f_1 = f_3 = f_4 = 0; \quad f_2 = 100; \quad L = 127.0 \text{ cm } (50 \text{ in.})\right]$

(a) SI Units

$\frac{N_x}{L}$, kPa	$\frac{W}{bL^2}$, kg/m^3	b_1, cm	b_2, cm	b_3, cm	b_4, cm	t_1, cm	t_2, cm	t_3, cm	t_4, cm
6895	143.8×10^{-1}	3.404	6.401	3.099	1.651	0.549	0.102	1.082	0.025
5516	124.4	3.810	6.502	1.930	1.854	.500	.102	1.270	.069
3448	91.2	3.378	6.350	1.270	2.565	.447	.097	1.270	.025
2758	83.5	3.378	5.563	3.175	2.743	.287	.084	.559	.178
2069	69.1	2.972	4.826	2.540	1.651	.203	.064	.356	.025
1379	55.9	2.718	4.724	.762	1.600	.206	.058	1.245	.036
690	40.1	2.362	4.013	.762	1.448	.147	.043	.737	.036
345	28.5	1.905	3.835	.762	1.168	.107	.041	.267	.025

(b) U.S. Customary Units

$\frac{N_x}{L}$, psi	$\frac{W}{bL^2}$, lb/in^3	b_1, in.	b_2, in.	b_3, in.	b_4, in.	t_1, in.	t_2, in.	t_3, in.	t_4, in.
1000	5.200×10^{-4}	1.340	2.520	1.220	0.650	0.216	0.040	0.426	0.010
800	4.500	1.500	2.560	.760	.730	.197	.040	.500	.027
500	3.300	1.330	2.500	.500	1.010	.176	.038	.500	.010
400	3.020	1.330	2.190	1.250	1.080	.113	.033	.220	.070
300	2.500	1.170	1.900	1.000	.650	.080	.025	.140	.010
200	2.020	1.070	1.860	.300	.630	.081	.023	.490	.014
100	1.450	.930	1.580	.300	.570	.058	.017	.290	.014
50	1.030	.750	1.510	.300	.460	.042	.016	.105	.010

TABLE 5.- OPTIMIZED DESIGN VARIABLES FOR GRAPHITE-EPOXY PANEL

$\left[f_1 = f_2 = 100; \quad f_3 = f_4 = 0; \quad L = 76.2 \text{ cm (30 in.)}\right]$

(a) SI Units

$\frac{N_x}{L}$, kPa	$\frac{W}{bL^2}$, kg/m^3	b_1, cm	b_2, cm	b_3, cm	b_4, cm	t_1, cm	t_2, cm	t_3, cm	t_4, cm
3448	92.6×10^{-1}	2.718	4.267	1.397	2.337	0.053	0.071	1.270	0.173
2758	81.6	4.318	4.115	3.861	2.540	.084	.076	.434	.163
2069	66.4	4.140	4.140	1.626	2.159	.051	.081	.549	.152
1379	57.5	2.350	3.277	2.108	2.388	.038	.051	.345	.152
690	39.0	2.197	2.946	.762	1.712	.036	.041	.470	.091
345	27.4	1.999	2.565	1.651	1.321	.025	.033	.127	.058

(b) U.S. Customary Units

$\frac{N_x}{L}$, psi	$\frac{W}{bL^2}$, lb/in^3	b_1, in.	b_2, in.	b_3, in.	b_4, in.	t_1, in.	t_2, in.	t_3, in.	t_4, in.
500	3.350×10^{-4}	1.070	1.680	0.550	0.920	0.021	0.028	0.500	0.068
400	2.950	1.700	1.620	1.520	1.000	.033	.030	.171	.064
300	2.400	1.630	1.630	.640	.850	.02	.032	.216	.060
200	2.080	.925	1.290	.830	.940	.015	.020	.136	.060
100	1.410	.865	1.160	.300	.674	.014	.016	.185	.036
50	.990	.787	1.010	.650	.520	.010	.013	.050	.023

TABLE 6.- OPTIMIZED DESIGN VARIABLES FOR GRAPHITE-EPOXY PANEL

$\left[f_1 = f_2 = 100; \quad f_3 = f_4 = 0; \quad L = 101.6 \text{ cm } (40 \text{ in.})\right]$

(a) SI Units

$\frac{N_x}{L}$, kPa	$\frac{W}{bL^2}$, kg/m^3	b_1, cm	b_2, cm	b_3, cm	b_4, cm	t_1, cm	t_2, cm	t_3, cm	t_4, cm
3448	92.6×10^{-1}	5.867	5.537	3.454	3.937	0.122	0.097	1.194	0.257
2758	83.5	4.115	5.512	2.972	2.997	.079	.094	.892	.206
2069	67.7	5.004	5.283	4.064	2.972	.097	.097	.437	.191
1379	55.9	2.972	4.699	2.032	2.489	.053	.076	.508	.163
690	39.5	3.810	4.089	3.073	2.083	.066	.058	.239	.089
345	27.5	2.565	3.378	1.499	1.829	.033	.041	.249	.081

(b) U.S. Customary Units

$\frac{N_x}{L}$, psi	$\frac{W}{bL^2}$, lb/in^3	b_1, in.	b_2, in.	b_3, in.	b_4, in.	t_1, in.	t_2, in.	t_3, in.	t_4, in.
500	3.350×10^{-4}	2.310	2.180	1.360	1.550	0.048	0.038	0.470	0.101
400	3.020	1.620	2.170	1.170	1.180	.031	.037	.351	.081
300	2.450	1.970	2.080	1.600	1.170	.038	.038	.172	.075
200	2.020	1.170	1.850	.800	.980	.021	.030	.200	.064
100	1.430	1.500	1.610	1.210	.820	.026	.023	.094	.035
50	.995	1.010	1.330	.590	.720	.013	.016	.098	.032

TABLE 7.- OPTIMIZED DESIGN VARIABLES FOR GRAPHITE-EPOXY PANEL

$\left[f_1 = f_2 = 100; \quad f_3 = f_4 = 0; \quad L = 127.0 \text{ cm } (50 \text{ in.})\right]$

(a) SI Units

$\frac{N_x}{L}$, kPa	$\frac{W}{bL^2}$, kg/m^3	b_1, cm	b_2, cm	b_3, cm	b_4, cm	t_1, cm	t_2, cm	t_3, cm	t_4, cm
3448	91.8×10^{-1}	6.096	6.731	3.810	3.912	0.076	0.102	0.610	0.203
2758	82.7	5.055	7.010	2.921	3.531	.130	.124	1.270	.213
2069	69.7	7.137	7.112	4.699	2.972	.165	.132	.643	.122
1379	55.9	3.099	5.461	4.750	3.454	.053	.084	.457	.216
690	40.1	4.115	4.674	3.861	2.946	.076	.058	.361	.117
345	27.7	4.623	4.267	2.464	2.337	.058	.053	.312	.086

(b) U.S. Customary Units

$\frac{N_x}{L}$, psi	$\frac{W}{bL^2}$, lb/in^3	b_1, in.	b_2, in.	b_3, in.	b_4, in.	t_1, in.	t_2, in.	t_3, in.	t_4, in.
500	3.320×10^{-4}	2.400	2.650	1.500	1.540	0.030	0.040	0.240	0.080
400	2.990	1.990	2.760	1.150	1.390	.051	.049	.500	.084
300	2.520	2.810	2.800	1.850	1.170	.065	.052	.253	.048
200	2.020	1.220	2.150	1.870	1.360	.021	.033	.180	.085
100	1.450	1.620	1.840	1.520	1.160	.030	.023	.142	.046
50	1.000	1.820	1.680	.970	.920	.023	.021	.123	.034

TABLE 8.- OPTIMIZED DESIGN VARIABLES FOR ALL-ALUMINUM PANEL WITH L = 76.2 cm (30 in.)

(a) SI Units

$\frac{N_x}{L}$, kPa	$\frac{W}{bL^2}$, kg/m^3	b_1, cm	b_2, cm	b_3, cm	b_4, cm	t_1, cm	t_2, cm	t_3, cm	t_4, cm
3448	230.3×10^{-1}	8.687	4.097	7.518	4.775	0.353	0.147	0.505	0.025
2758	185.8	7.239	4.242	6.782	3.924	.284	.160	.287	.025
2069	153.7	6.142	4.191	5.525	3.404	.231	.150	.208	.025
1379	123.0	4.572	3.744	4.432	2.642	.157	.122	.074	.025
690	87.1	4.343	3.226	3.912	2.591	.124	.089	.117	.025
345	61.1	3.061	2.787	2.946	2.057	.074	.066	.074	.025

(b) U.S. Customary Units

$\frac{N_x}{L}$, psi	$\frac{W}{bL^2}$, lb/in^3	b_1, in.	b_2, in.	b_3, in.	b_4, in.	t_1, in.	t_2, in.	t_3, in.	t_4, in.
500	8.330×10^{-4}	3.420	1.613	2.960	1.880	0.139	0.058	0.199	0.010
400	6.720	2.850	1.670	2.670	1.545	.112	.063	.113	.010
300	5.560	2.418	1.650	2.175	1.340	.091	.059	.082	.010
200	4.450	1.800	1.474	1.745	1.040	.062	.048	.069	.010
100	3.150	1.710	1.270	1.540	1.020	.049	.035	.046	.010
50	2.210	1.205	1.097	1.160	.810	.029	.026	.029	.010

TABLE 9.- OPTIMIZED DESIGN VARIABLES FOR GRAPHITE-EPOXY PANEL

WITH PRACTICAL CONSTRAINTS

$\left[f_1 = f_3 = f_4 = 0; \quad f_2 = 100; \quad L = 76.2 \text{ cm (30 in.)}\right]$

(a) SI Units

$\frac{N_x}{L}$, kPa	$\frac{W}{bL^2}$, kg/m^3	b_1, cm	b_2, cm	b_3, cm	b_4, cm	t_1, cm	t_2, cm	t_3, cm	t_4, cm
3448	92.4×10^{-1}	3.355	4.044	2.289	3.970	0.065	0.072	0.569	0.276
2758	82.9	3.091	3.833	1.869	3.241	.060	.068	.632	.182
2069	72.1	3.719	3.584	1.687	3.155	.067	.060	.620	.170
1379	59.1	1.918	3.119	.869	2.360	.030	.044	.635	.153
690	40.4	1.806	2.786	.772	2.090	.025	.036	.414	.088
345	28.7	2.065	2.441	.780	1.966	.025	.037	.270	.057

(b) U.S. Customary Units

$\frac{N_x}{L}$, psi	$\frac{W}{bL^2}$, lb/in^3	b_1, in.	b_2, in.	b_3, in.	b_4, in.	t_1, in.	t_2, in.	t_3, in.	t_4, in.
500	3.338×10^{-4}	1.321	1.592	0.901	1.563	0.0257	0.0285	0.2240	0.1088
400	2.997	1.217	1.509	.736	1.276	.0236	.0267	.2487	.0717
300	2.607	1.464	1.411	.664	1.242	.0265	.0237	.2440	.0669
200	2.136	.755	1.228	.342	.929	.0118	.0172	.2500	.0603
100	1.462	.711	1.097	.304	.823	.0100	.0144	.1630	.0345
50	1.037	.813	.961	.307	.774	.0100	.0147	.1063	.0224

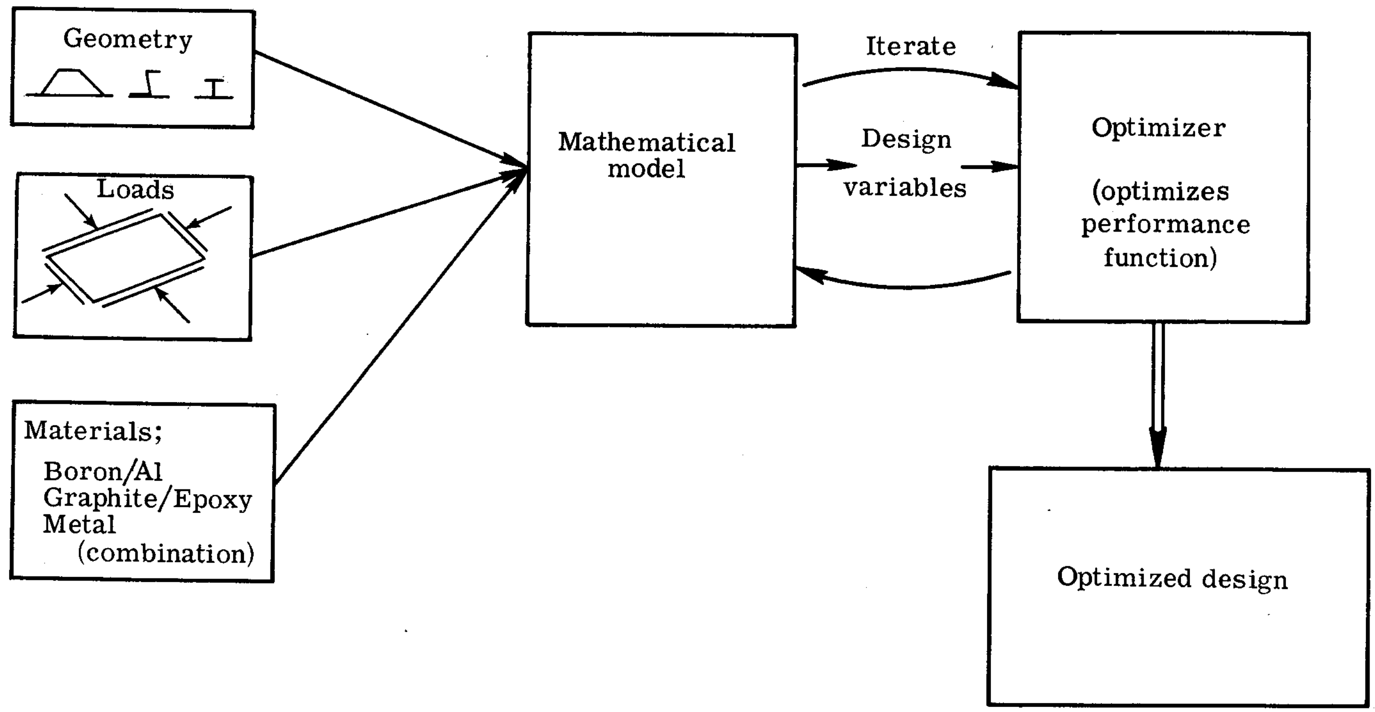

Figure 1.- Optimization cycle.

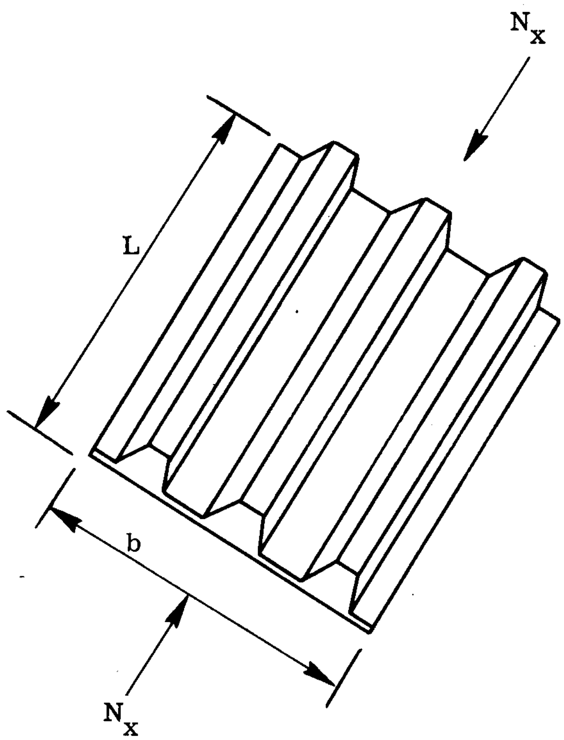

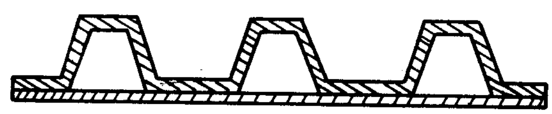

Cross section

Figure 2.- Panel to be optimized.

Design Variables

t_i	4
b_i	4
f_i	4
Total Number = 12	

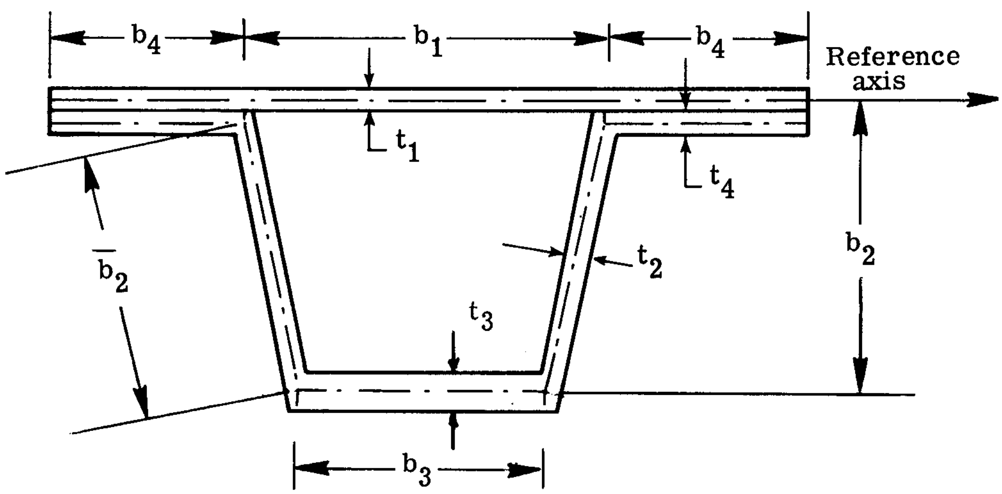

Figure 3.- Representative cross section of the idealized panel.

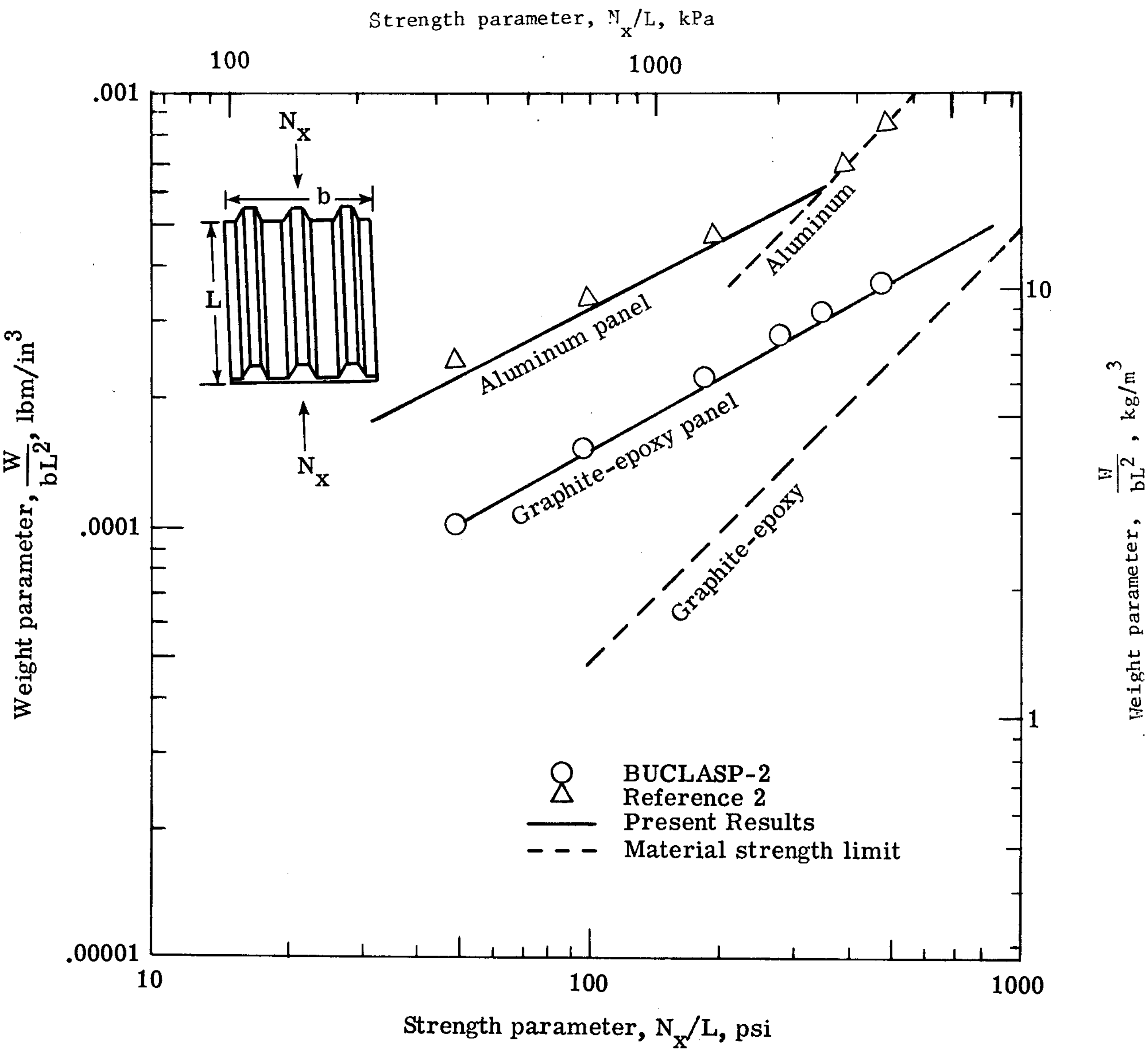

Figure 4.- Weight-strength plot for graphite-epoxy and aluminum panels.

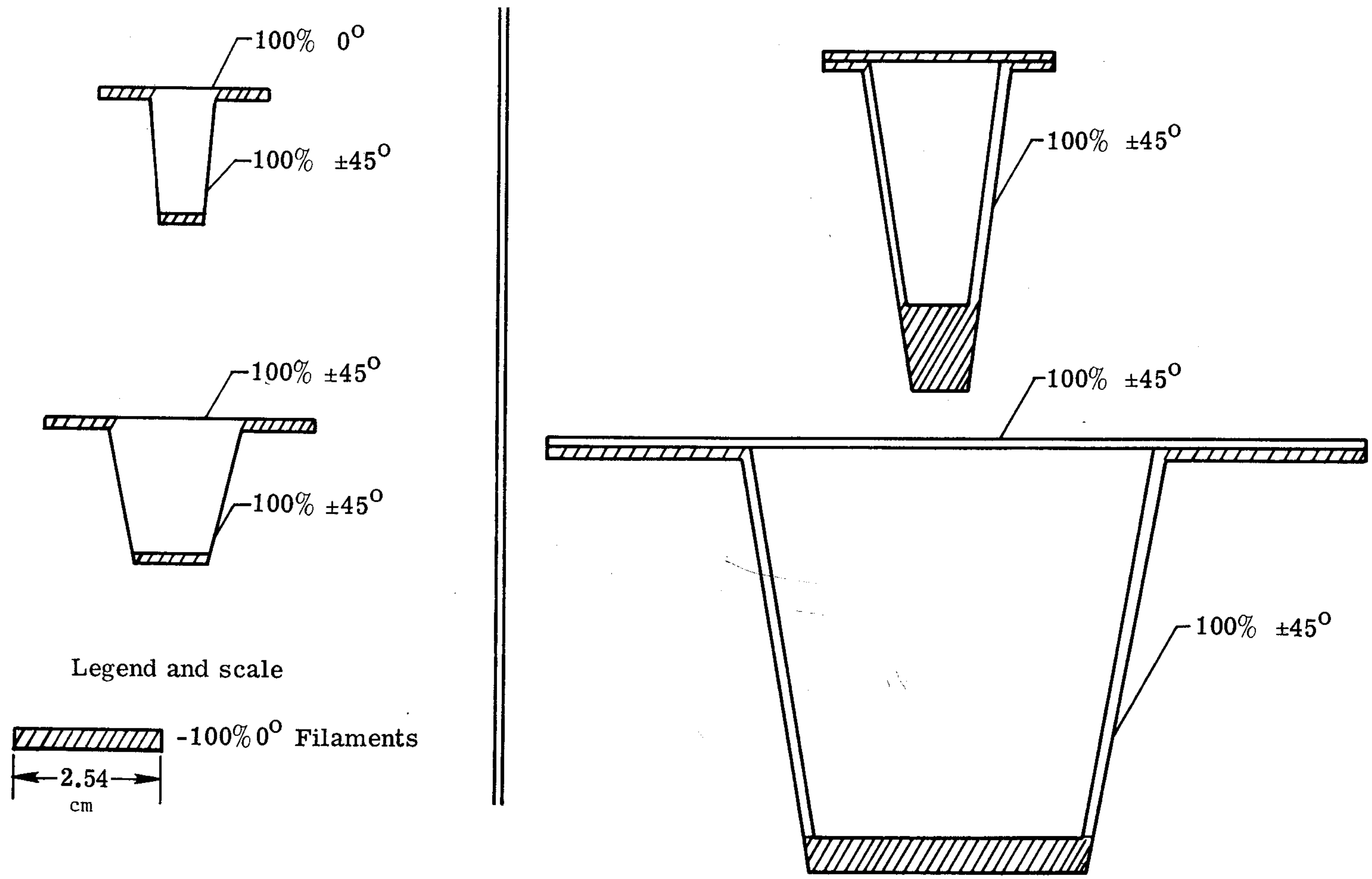

(a) Lightly loaded (N_x/L = 345 kPa).

(b) Heavily loaded (N_x/L = 3448 kPa).

Figure 5.- Examples of optimized graphite-epoxy sections.

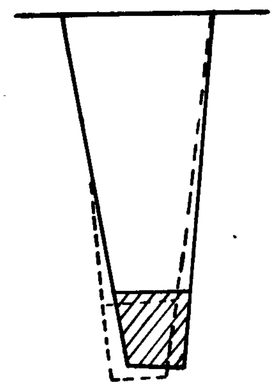

(a) Antisymmetric mode.

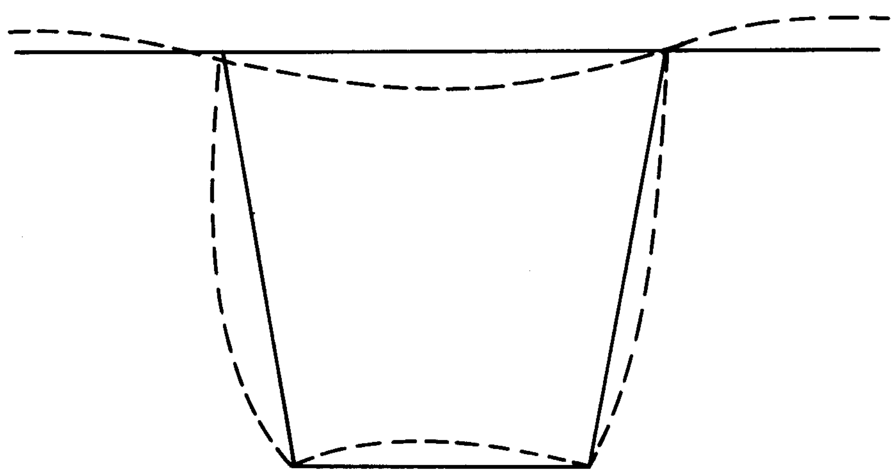

(b) Symmetric mode.

Figure 6.- BUCLASP-2 buckling modes for heavily loaded panel (N_x/L = 3448 kPa).

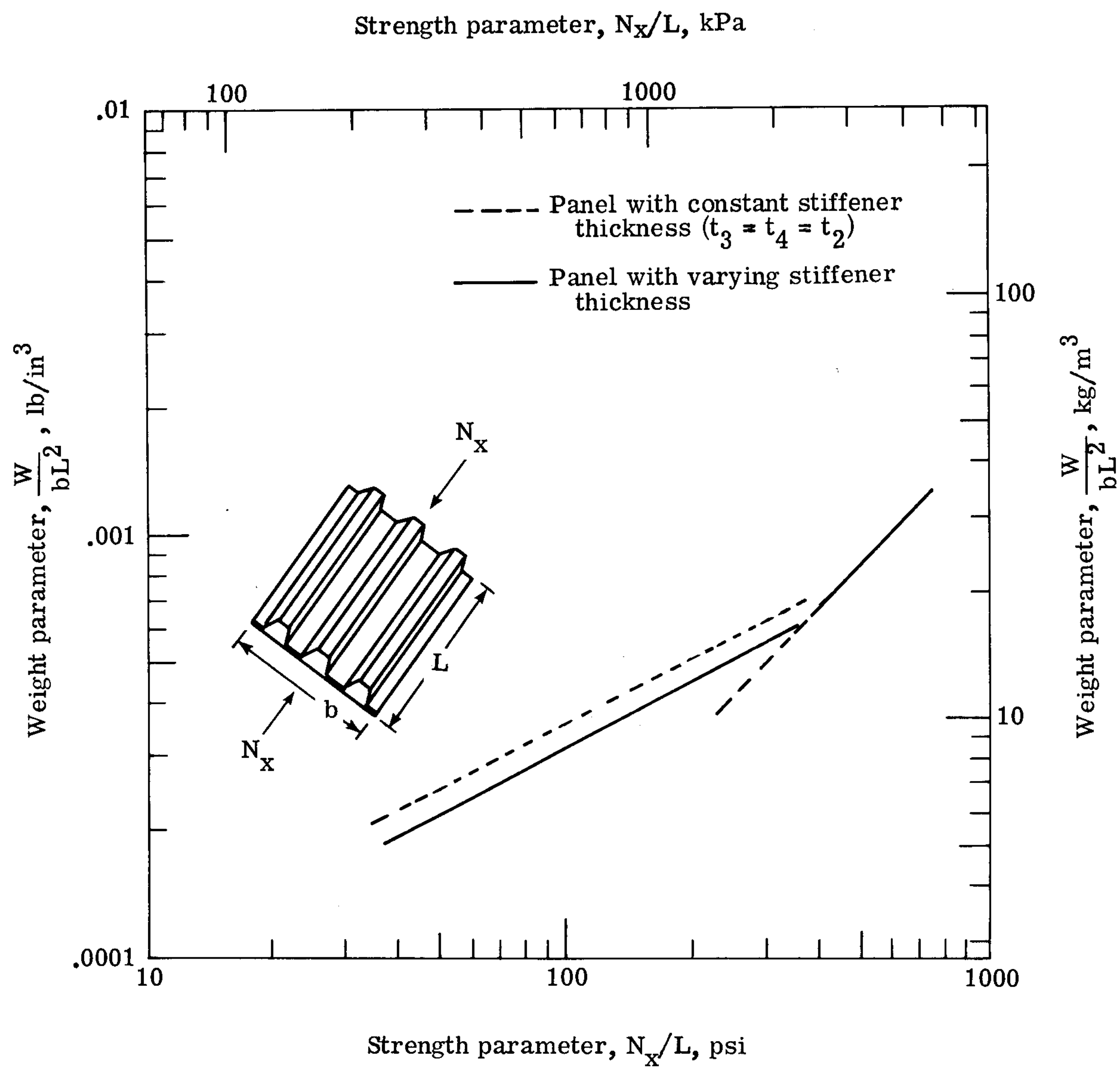

Figure 7.- Effect of varying stiffener thickness on aluminum panel.

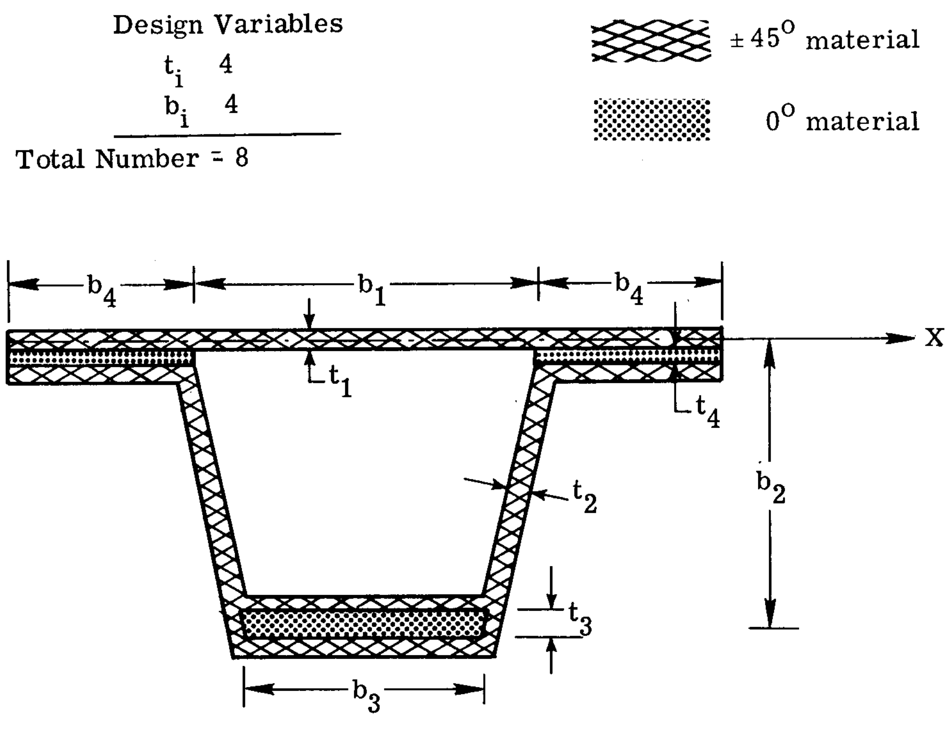

Figure 8.- Representative cross section of the panel with practical constraints.

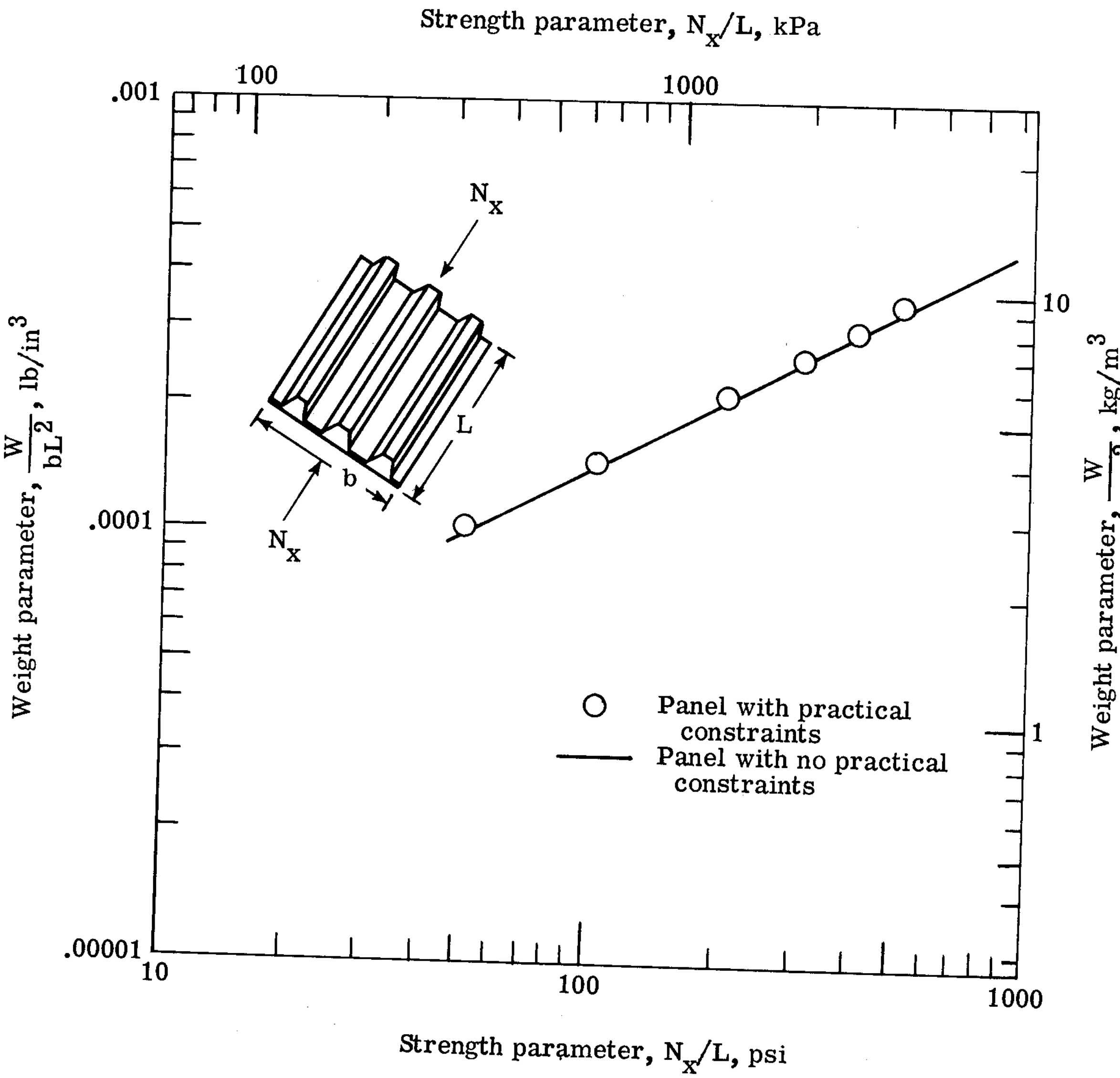

Figure 9.- Effect of practical constraints on graphite-epoxy panel.

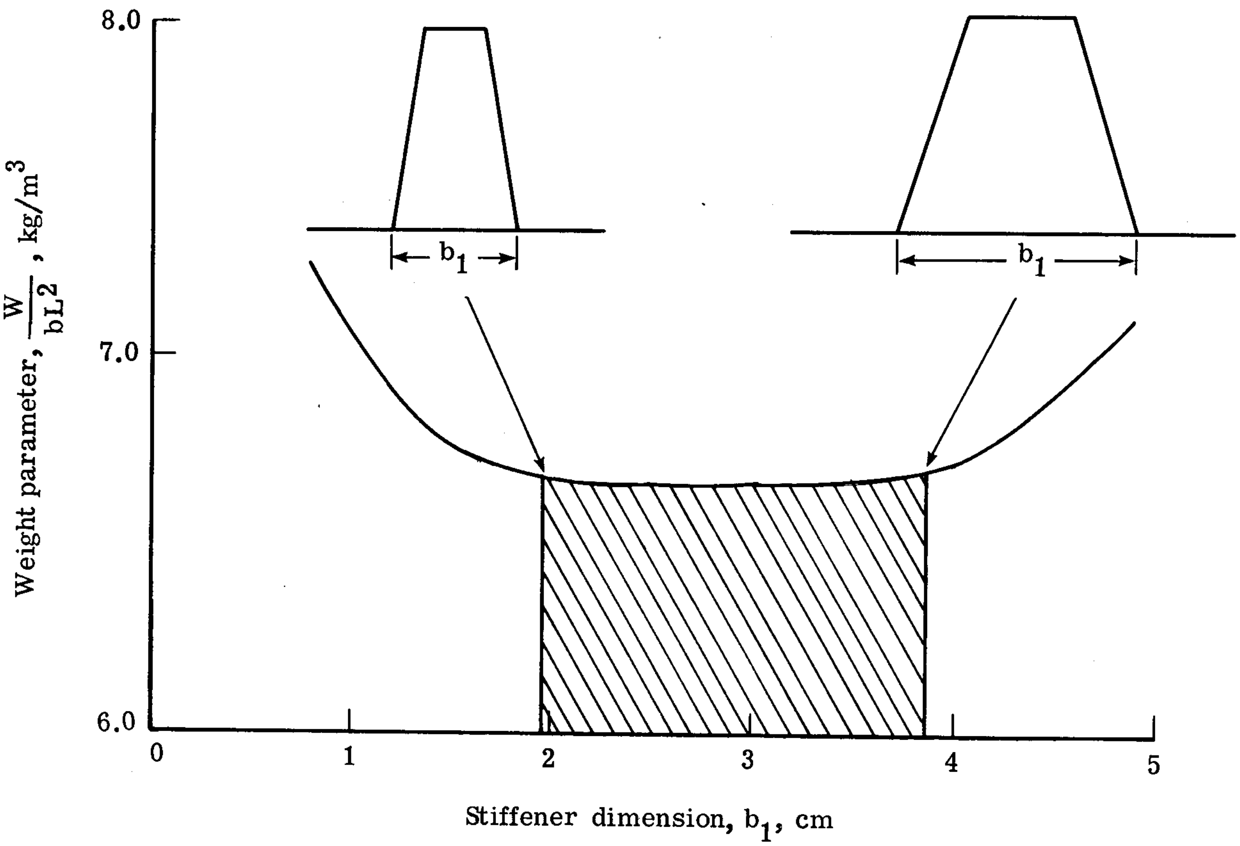

Figure 10.- Weight-parameter sensitivity with respect to varying b_1.
$\frac{N_x}{L}$ = 2069 kPa; L = 76.2 cm.

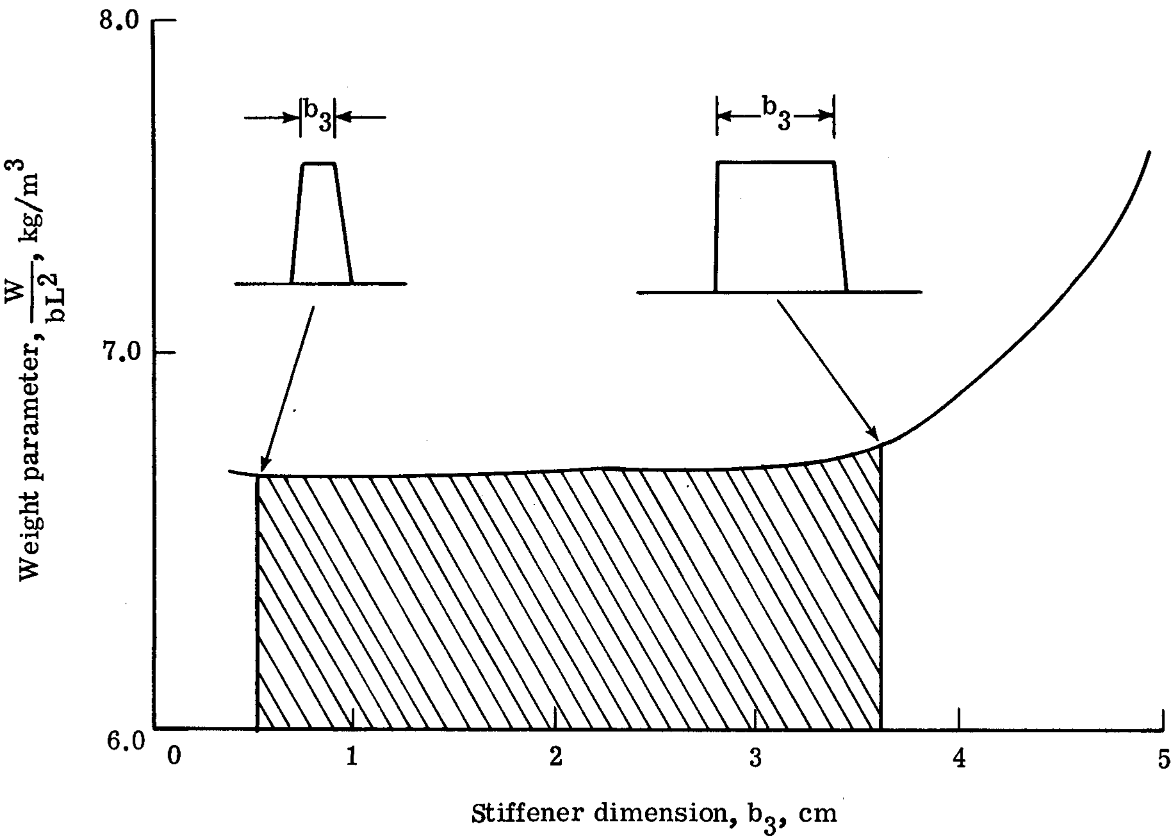

Figure 11.- Weight-parameter sensitivity with respect to varying b_3.
$\frac{N_x}{L}$ = 2069 kPa; L = 76.2 cm.

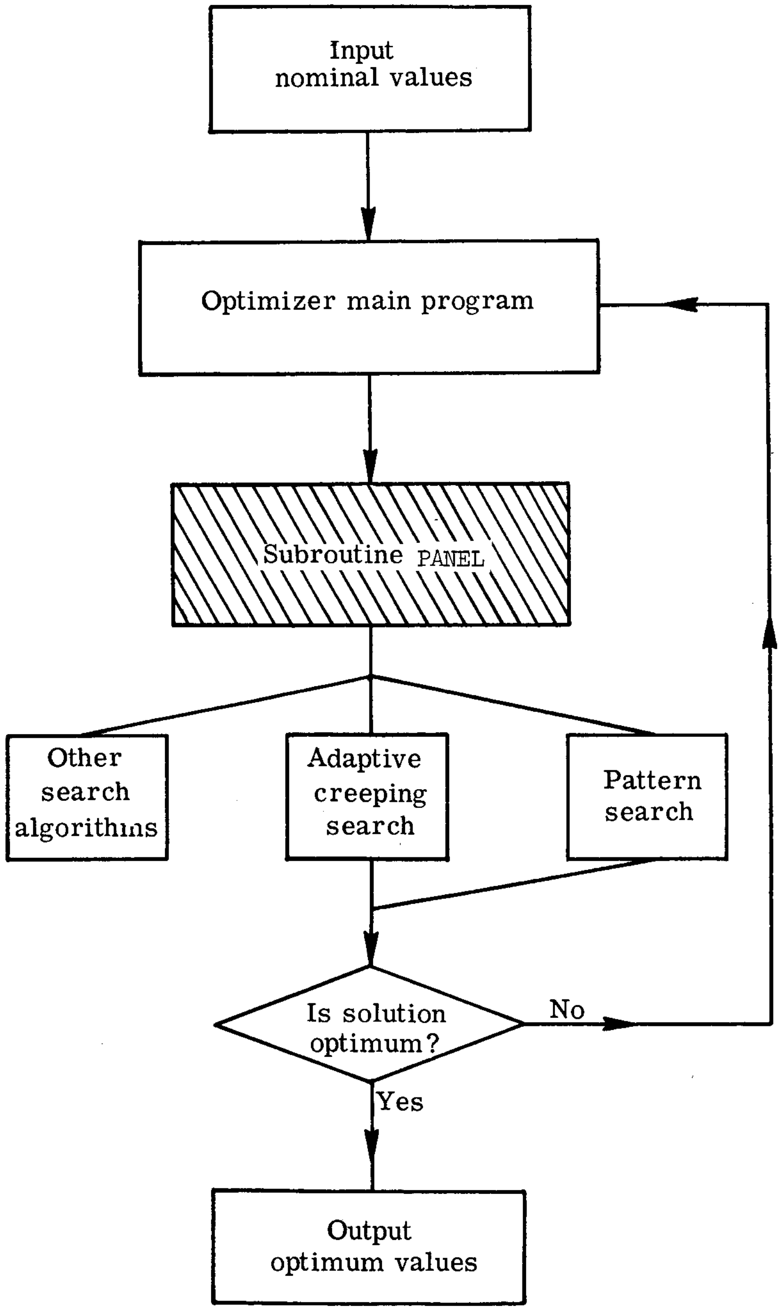

Figure 12.- Flow chart for optimization program.

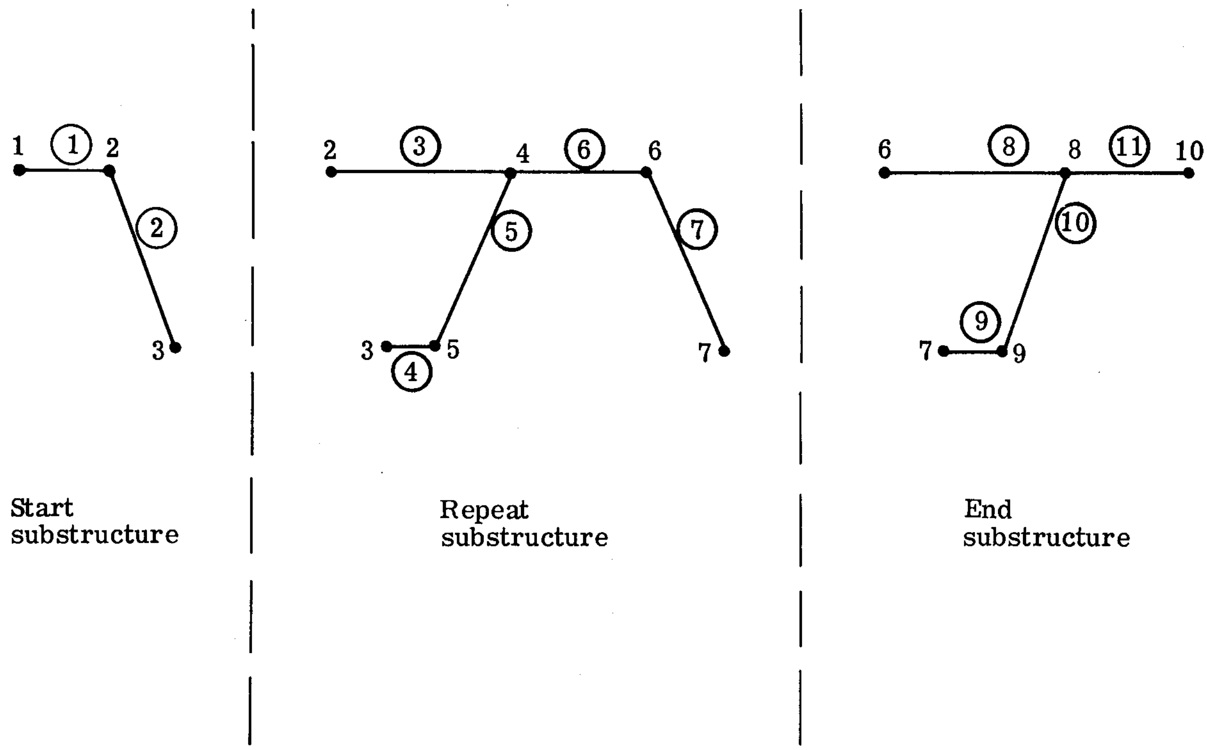

Figure 13.- Mathematical model for BUCLASP-2.

NASA-Langley, 1974 L-9739